Article:
YULE, GREGORY, Taylor, Daniel Aaron, Hedges, Jonathan et al. (2026) Enhanced signal discrimination for mixture analysis using SABRE hyperpolarised benchtop 1H NMR spectroscopy. Chemical communications. ISSN: 1364-548X

https://doi.org/10.1039/d6cc03999e

ChemComm

ROYAL SOCIETY OF CHEMISTRY

COMMUNICATION

Published on 28 July 2026

Cite this: DOI: 10.1039/d6cc03999e

Received 23rd June 2026,
Accepted 27th July 2026

DOI: 10.1039/d6cc03999e

rsc.li/chemcomm

Enhanced signal discrimination for mixture analysis using SABRE hyperpolarised benchtop ^{1}H NMR spectroscopy

Gregory J. Yule, [a] Daniel A. Taylor, [a] Jonathan Hedges[b] and Meghan E. Halse *[a]

^{1}H benchtop NMR spectroscopy provides a more accessible alternative to high-field NMR but suffers from lower sensitivity and increased peak overlap. Here, we overcome these challenges by combining SABRE hyperpolarisation with homonuclear decoupling and ultra-selective pulse sequences. The efficacy of this approach is demonstrated for a mixture of analytes, where the 700-fold signal enhancement provided by SABRE enables the acquisition of a well-resolved homodecoupled ^{1}H benchtop NMR spectrum, along with sub-spectra for each component, extracted from a region of significant peak overlap.

Benchtop NMR spectrometers, with magnetic field strengths of B_0 = 1–2 T, offer a more accessible alternative to high-field NMR ($B_0 \geq 7$ T), with benefits such as lower purchase and maintenance costs, greater portability, and no requirement for cryogens. However, these benefits come with drawbacks, most notably reduced sensitivity and increased peak overlap, particularly for ^{1}H NMR, where a narrow chemical shift range compounds the overlap issues and often leads to significant strong coupling effects.

A range of hyperpolarisation techniques have been used to boost the sensitivity of benchtop NMR spectroscopy, showing potential for analytical applications ranging from reaction monitoring and complex mixture analysis to high-throughput drug screening.[1,2] By utilising sources of high spin order, non-Boltzmann spin populations are generated in the target molecule(s),[3] breaking the link between NMR sensitivity and detection field strength. In the *para*hydrogen-induced polarisation (PHIP) method,[4,5] the source of spin order is the NMR-silent nuclear singlet state of dihydrogen, *para*hydrogen (pH$_2$). Signal amplification by reversible exchange (SABRE)[6] is a catalytic method of transferring the spin order of pH$_2$ to a target analyte, while reversibly bound to a transition metal catalyst, typically iridium, in the presence of a weak magnetic field (*ca.* 6.5 mT for transfer to ^{1}H). Reversible exchange of both pH$_2$ and the target builds up hyperpolarisation of the analyte in free solution over a period of a few seconds. Orders-of-magnitude signal enhancements are observed following sample transfer into the NMR spectrometer for detection. SABRE has been combined with benchtop NMR to enhance a range of nuclei including ^{1}H, ^{19}F, ^{15}N, and ^{13}C,[7–11] reducing limits of detection and enabling quantification into the micromolar to millimolar range.[12,13] SABRE hyperpolarisation can be repeatedly regenerated as long as fresh pH$_2$ is supplied. A range of automated workflows have been developed to produce repeatable hyperpolarisation within the recycle delay of multi-step NMR experiments.[7,14–19]

For mixture analysis, signal overlap in ^{1}H benchtop NMR spectra must also be addressed. Homonuclear decoupling can be used to collapse signal multiplicity into one well-resolved singlet for each chemical environment (in the absence of heteronuclear coupling).[20,21] Liquid-state homonuclear decoupling can be achieved using interferogram,[22] real-time,[23] or semi-real-time[24] pure shift methods, in which J-evolution is repeatedly refocused[22,25–27] and the free induction decay (FID) is acquired in chunks. An alternative approach, 2D J-resolved spectroscopy (JRES), encodes scalar coupling information into the indirect dimension of a 2D experiment.[28] The homodecoupled ^{1}H NMR spectrum is then obtained following a 45° projection. Mandral *et al.* compared the performance of interferogram pure shift and JRES methods on a benchtop NMR spectrometer.[29] They found that the overall optimal sensitivity performance was achieved for the JRES approach, while the Zangger–Sterk (ZS) refocusing element[30] provided the best sensitivity out of the interferogram methods.

To date, only real-time pure shift has been combined with hyperpolarisation,[31,32] owing to its ability to obtain a homonuclear decoupled FID in a single experiment. In practice, the resolution of real-time pure shift methods is limited by the duration of the repeated refocusing element, which can be

[a] *Department of Chemistry, University of York, Heslington, York, North Yorkshire, YO10 5DD, UK. E-mail: meghan.halse@york.ac.uk*
[b] *Research IT, University of York, Heslington, York, North Yorkshire, YO10 5DD, UK*

quite long due to the narrow spectral widths of ^{1}H benchtop NMR spectra. Therefore, it is desirable to have a renewable source of hyperpolarisation that can be combined with the interferogram and JRES methods.

While homonuclear decoupling simplifies the entire spectrum, peak overlap can still occur. A complementary approach is to use ultra-selective experiments, such as GEMSTONE (Gradient Enhanced Multiplet Selective Targeted Observation NMR Experiment)[33] or DREAMTIME (Designed Refocused Excitation And optional Mixing for Targets *In vivo* and Mixture Elucidation),[34] to excite a resonance or spin system of interest from a region of peak overlap. Both GEMSTONE and DREAMTIME have been implemented on a benchtop NMR spectrometer previously[35] but only DREAMTIME with high-field NMR detection has been combined with SABRE.[36]

In this work, we demonstrate the combination of automated SABRE hyperpolarisation with homodecoupled ^{1}H benchtop NMR to deliver enhanced signal discrimination of mixtures. We report the first implementation of SABRE-enhanced GEMSTONE to extract single resonances from regions of spectral overlap and compare the performance of hyphenated GEMSTONE techniques (GEMSTONE-TOCSY[37] and GEMSTONE-CLIP-COSY[38]) for selectively transferring polarisation to a wider spin system.

For all experiments presented herein, SABRE hyperpolarisation is generated using a previously described automated workflow.[19] The sample is re-polarised within the recycle delay of the relevant NMR experiment by shuttling the sample to an *ex situ* polarisation transfer field, bubbling pH$_2$ through the solution, and then returning the sample to the NMR spectrometer for detection. Each generation of hyperpolarisation takes *ca.* 13 s.

The SABRE-enhanced ^{1}H benchtop (80 MHz) NMR spectrum of a four-component mixture of 1 mM each of 4-methylpyridine (4-mPy), pyridine (Py), 3,5-dimethylpyridine (3,5-mPy), and 1-methyl-1*H*-1,2,3-triazole (mtz) presented in Fig. 1a exhibits strong hyperpolarisation for all components, with an average enhancement factor of 700-fold across the aromatic region of the spectrum. However, the spectrum suffers from significant peak overlap, illustrating the challenge of using ^{1}H benchtop NMR for mixture analysis.

The JRES experiment effectively removes the multiplet structure to produce nine distinct singlets in the aromatic region, with good signal-to-noise ratios and average linewidths of 2.5 Hz (single echo (SE), Fig. 1b) and 3.4 Hz (double echo (DE), Fig. 1c). Notably, the broadly overlapped multiplets arising from the *para* Py resonance and the aromatic protons of mtz, as well as the *meta* Py and *para* 3,5-mPy resonances, are resolved.

The DE variant of the JRES experiment is expected to be more robust against strong coupling effects. However, no significant improvement in the level of observable artefacts (red asterisks) is achieved using the DE compared to the SE JRES sequence (Fig. 1). The quality of the SE and DE JRES spectra are comparable, with a moderately improved performance for the SE sequence in terms of average linewidth (Table S4), while the

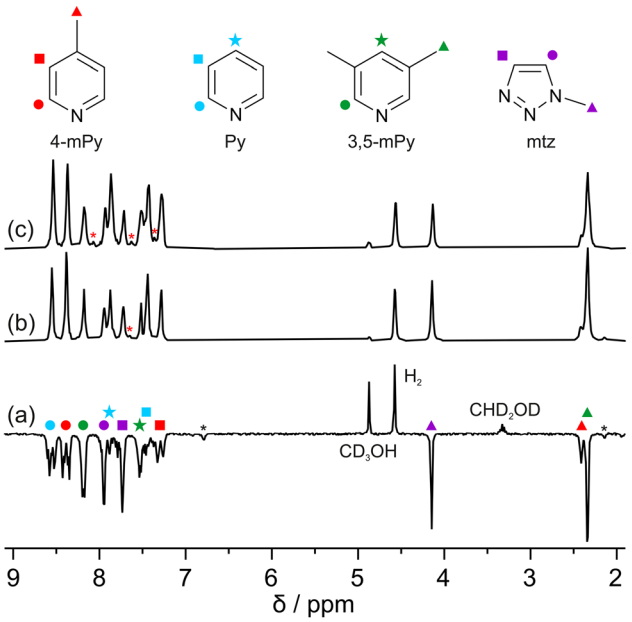

Fig. 1 SABRE-hyperpolarised ^{1}H benchtop NMR spectra of a four-component mixture containing 1 mM each of pyridine, 4-methylpyridine, 3,5-dimethylpyridine, and 1-methyl-1*H*-1,2,3-triazole with SABRE pre-catalyst [IrCl(COD)(IMes)] (100 μM) in methanol-d$_4$ under 2 bar absolute pH$_2$. Spectra were acquired with: (a) ^{1}H pulse acquire, 1 scan, (b) single-echo (SE) JRES, and (c) double-echo (DE) JRES. JRES spectra were acquired in a single scan with 32 steps and a 20 Hz bandwidth in the indirect dimension for a total experiment time of 11 min. Artefacts are denoted by red asterisks and catalyst resonances are denoted by black asterisks.

DE sequence provided higher signal retention (Table S5). SABRE-enhanced JRES experiments were repeated on a single-component sample of pyridine, which is expected to exhibit the most significant strong coupling effects of the four components in the mixture (Fig. S5 in the SI). As in Fig. 1, no significant difference in the number or prominence of artefacts was observed in the SABRE-enhanced SE and DE JRES benchtop NMR spectra of pyridine. Therefore, we conclude that strong coupling does not play a significant role for these analytes at 80 MHz.

SABRE-enhanced ZS interferogram pure shift ^{1}H NMR spectra were also acquired of the four-component mixture (Fig. S6) and pyridine (Fig. S5). Significant sensitivity losses were observed for the interferogram ZS approach (*ca.* 7% of signal retained relative to ^{1}H pulse acquire). While sensitivity was improved by narrowing the bandwidth to include just the aromatic region, only *ca.* 22% of the signal was retained with an average linewidth of 4.7 Hz. A summary of the relative performance of the JRES and ZS methods in terms of linewidth reduction (Table S4) and signal retention (Table S5) is provided in the SI.

The narrow chemical shift range of ^{1}H benchtop NMR leads to peak overlap even in homodecoupled ^{1}H NMR spectra (Fig. 1). Ultra-selective observation experiments can be used to obtain a spectrum containing only the resonance or spin system of interest. A key parameter for optimisation of selective pulse sequences such as GEMSTONE is the precise chemical

shift of the target resonance. Therefore, a homodecoupled ^{1}H NMR spectrum is a necessary first step to implementing optimised ultra-selective pulse sequences.

Fig. 2 presents a set of SABRE-enhanced GEMSTONE ^{1}H benchtop NMR spectra (8 scans, 3 min each) of the four-component mixture, where each experiment has been optimised to extract a single resonance from the overlapped aromatic region. The optimised GEMSTONE parameters are reported in the SI. A requirement of GEMSTONE is that the selective pulse applied to the target resonance must have a bandwidth that is sufficiently narrow such that none of its coupling partners are excited. In the case of the *para* and *meta* resonances of pyridine, separated by only 34.5 Hz on the 80 MHz benchtop NMR spectrometer, this is not feasible. Therefore GEMSTONE spectra cannot be acquired of the *para* and *meta* resonances. However, the *ortho* resonance of pyridine is sufficiently separated to be amenable to GEMSTONE with a 40 Hz (86.2 ms) selective pulse.

The selectivity of GEMSTONE is improved by increasing the duration of the frequency swept pulses, at the cost of sensitivity losses due to relaxation and diffusion. This compromise between sensitivity and selectivity is most evident in the GEMSTONE spectrum of the *para* resonance of 3,5-dimethylpyridine. Due to the overlap with one of the resonances of pyridine, a long adiabatic pulse duration of 100 ms was required to achieve the desired level of selectivity, giving rise to noticeably weaker signal. We note that a new pulse sequence, JND-GEMSTONE,[39] has recently been published by Bazzoni *et al.*, which replaces each frequency swept adiabatic pulse in GEMSTONE with multiple pairs of shorter pulses, to counter the sensitivity losses due to diffusion. This new, more sensitive approach is expected to be particularly advantageous for benchtop NMR applications, where the separation between peaks in Hz is much smaller than at high field. While some preliminary experiments have shown promise, a full evaluation of this new pulse sequence is beyond the scope of this communication.

GEMSTONE can be combined with other NMR pulse sequences to selectively target a spin system rather than a single resonance.[33,37,38] Fig. 3a presents a series of SABRE-enhanced GEMSTONE-TOCSY spectra (8 scans, 3 min each) targeting individual components of the mixture. The peak selected by the GEMSTONE sequence is indicated by the arrow. While GEMSTONE-TOCSY is able to transfer the hyperpolarisation across the spin system in each case, significant artefacts are observed at the chemical shifts of the other components of the mixture, particularly in the GEMSTONE-TOCSY spectra targeting pyridine and 4-methylpyridine. SABRE-enhanced GEMSTONE-COSY benchtop NMR spectra (Fig. S8 in the SI) contain fewer artefacts but feature anti-phase peaks. This latter issue can be overcome through the use of the CLIP-COSY experiment.[38,40]

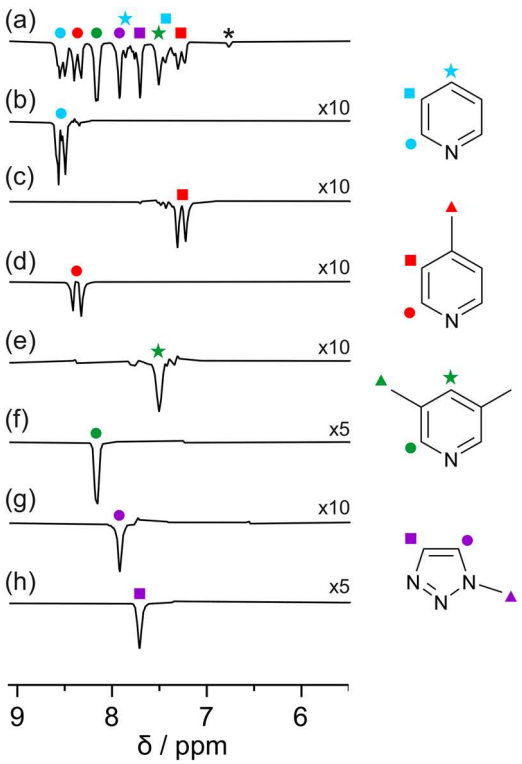

Fig. 2 SABRE-hyperpolarised ^{1}H NMR spectra (8 scans, 3 min each) of a mixture containing 1 mM each of pyridine, 4-methylpyridine, 3,5-dimethylpyridine, and 1-methyl-1*H*-1,2,3-triazole with the SABRE pre-catalyst ([IrCl(COD)(IMes)], 100 μM) in methanol-d_4 under 2 bar absolute pH_2. (a) ^{1}H pulse-acquire. (b)–(h) GEMSTONE spectra, where the bandwidth of the selective pulse and duration of the frequency swept adiabatic pulses were optimised separately for each target resonance and are provided in Table S1 in the SI.

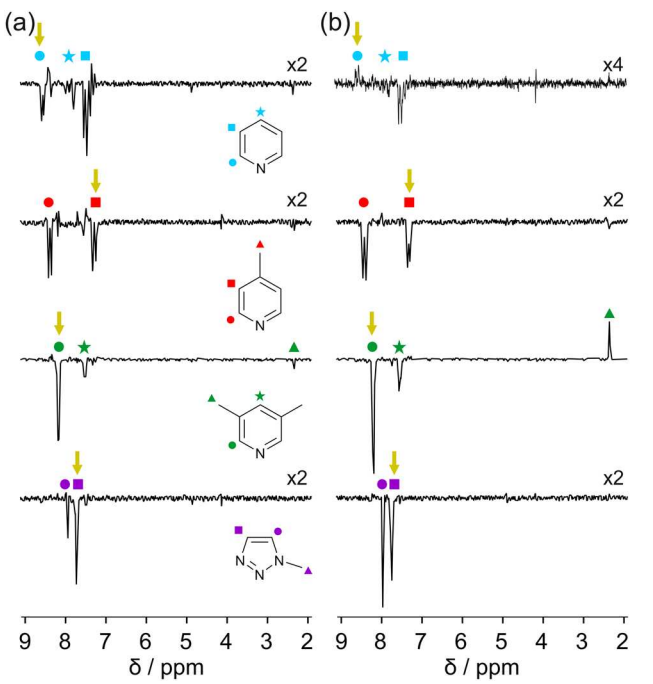

Fig. 3 SABRE-hyperpolarised (a) GEMSTONE-TOCSY and (b) GEMSTONE-CLIP-COSY benchtop NMR spectra (8 scans, 3 min each) of a mixture of pyridine, 4-methylpyridine, 3,5-dimethylpyridine, and mtz (1 mM each) with 100 μM of the SABRE pre-catalyst [IrCl(COD)(IMes)] in methanol-d_4 under 2 bar absolute pH_2. The arrows indicate the resonance targeted by the GEMSTONE sequence. The GEMSTONE parameters and mixing times were optimised individually for each target analyte and are provided in Table S1 in the SI.

The SABRE-enhanced GEMSTONE CLIP-COSY spectra targeting 4-mPy, 3,5-mPy, and mtz in Fig. 3b (8 scans, 3 min each) provide in-phase NMR spectra with improved SNR compared to the GEMSTONE-TOCSY spectra and fewer artefacts. By contrast, significant sensitivity losses were observed in the SABRE-enhanced GEMSTONE-CLIP-COSY spectrum of pyridine, with only 17% of the GEMSTONE signal retained. In this case, no single mixing time was found to enhance all three resonances with good SNR. The mixing time used here (70 ms) represents a compromise between sensitivity and signal distribution across the spin system. A comparison of the signal retention in the GEMSTONE-TOCSY and GEMSTONE-CLIP-COSY spectra is provided in Table S6 in the SI.

In conclusion, we have demonstrated that the combination of renewable SABRE hyperpolarisation with spectral simplification techniques can be used to overcome two challenges of ^{1}H benchtop NMR for complex mixture analysis: limited sensitivity and peak overlap. Specifically, we have implemented SABRE-enhanced homodecoupled ^{1}H benchtop NMR experiments, enabled by an automated SABRE hyperpolarisation workflow that delivers repeatable hyperpolarisation between each step of the experiment. The JRES sequence was found to provide the optimal performance for a four-component mixture (1 mM each) in a total experiment time of only 11 min. The ultra-selective NMR pulse sequence, GEMSTONE, was combined with SABRE for the first time, with the automated hyperpolarisation approach enabling phase cycling to minimise artefacts (*e.g.*, from the solvent). Hyphenated GEMSTONE techniques for enhancing spin systems, in addition to single resonances, were explored and it was found that GEMSTONE-CLIP-COSY provided the best selectivity and sensitivity with fewer artefacts when compared to GEMSTONE-TOCSY. However, a limitation of the GEMSTONE-CLIP-COSY approach is the availability of a suitable mixing time to enhance all resonances simultaneously. In the future, the performance of these hyphenated GEMSTONE techniques could be compared to SABRE-enhanced DREAMTIME, which isolates pairs of coupled resonances from region of peak overlap, as demonstrated previously by Norcott[36] using high-field detection.

The combination of SABRE with homonuclear decoupling and ultra-selective observation experiments can be used to enable the study of complex mixtures by ^{1}H benchtop NMR, for example in the analysis of metabolites in bio-fluids.[18] SABRE is a chemically selective method due to the fact that the target analyte needs to bind reversibly to the catalyst on a suitable timescale to be enhanced. Therefore, in a complex mixture only SABRE-active analytes will be enhanced. At the concentrations considered here, any non-hyperpolarised mixture components would have insufficient SNR to be observed in either the JRES or GEMSTONE NMR spectra without extensive signal averaging. However, the scope of SABRE-amenable analytes is being expanded through innovations in catalyst design,[41] the addition of co-substrate(s) to facilitate binding,[42] and the use of a polarisation transfer agent in the SABRE-Relay method to enable signal enhancement of analytes in solution (not bound to the catalyst) *via* proton exchange.[43]

Author contributions

G. J. Y.: conceptualisation, methodology, software, validation, formal analysis, investigation, data curation, writing – original draft, writing – review & editing, visualisation. D. A. T.: conceptualisation, methodology, software, writing – review and editing, project administration. J. H.: software, data curation. M. E. H.: conceptualisation, methodology, software, validation, formal analysis, investigation, resources, data curation, writing – original draft, writing – review & editing, visualisation, supervision, project administration, funding acquisition.

Conflicts of interest

There are no conflicts to declare.

Data availability

The data supporting this research is openly available from the research data repository of the University of York at DOI: https://doi.org/10.15124/554b6e41-8f95-460b-b1de-c7cb905c3dbc.

Ref. 44–49 have been cited in the supplementary information (SI). Supplementary information: full experimental details, additional NMR spectra. See DOI: https://doi.org/10.1039/d6cc03999e.

Acknowledgements

This research was supported by the UK Engineering and Physical Sciences Research Council (Grant Num: EP/X03528X/1 and EP/R028745/1). The authors thank Victoria Annis for the synthesis of the SABRE pre-catalyst, Izzy Hedges for carrying out preliminary experiments, Joris Mandral for providing example benchtop NMR pure shift pulse sequences, and Jean-Nicolas Dumez for helpful discussions on the implementation and optimisation of GEMSTONE.

References

1 M. Bütikofer, G. R. Stadler and F. Torres, *Chem.:Methods*, 2024, **4**, e202400009.
2 A. I. Silva Terra, D. A. Taylor and M. E. Halse, *Prog. Nucl. Magn. Reson. Spectrosc.*, 2024, **144–145**, 153–178.
3 J. Eills, D. Budker, S. Cavagnero, E. Y. Chekmenev, S. J. Elliott, S. Jannin, A. Lesage, J. Matysik, T. Meersmann, T. Prisner, J. A. Reimer, H. Yang and I. V. Koptyug, *Chem. Rev.*, 2023, **123**, 1417–1551.
4 J. Natterer and J. Bargon, *Prog. Nucl. Magn. Reson. Spectrosc.*, 1997, **31**, 293–315.
5 D. Golowicz, K. Kazimierczuk, M. Urbańczyk and T. Ratajczyk, *ChemistryOpen*, 2019, **8**, 196–200.
6 R. W. Adams, J. A. Aguilar, K. D. Atkinson, M. J. Cowley, P. I. P. Elliott, S. B. Duckett, G. G. R. Green, I. G. Khazal, J. Lopez-Serrano and D. C. Williamson, *Science*, 2009, **323**, 1708–1711.
7 P. M. Richardson, A. J. Parrott, O. Semenova, A. Nordon, S. B. Duckett and M. E. Halse, *Analyst*, 2018, **143**, 3442–3450.
8 P. M. Richardson, W. Iali, S. S. Roy, P. J. Rayner, M. E. Halse and S. B. Duckett, *Chem. Sci.*, 2019, **10**, 10607–10619.
9 J. F. P. Colell, M. Emondts, A. W. J. Logan, K. Shen, J. Bae, R. V. Shchepin, G. X. Ortiz, P. Spannring, Q. Wang, S. J. Malcolmson, E. Y. Chekmenev, M. C. Feiters, F. P. J. T. Rutjes,

B. Blümich, T. Theis and W. S. Warren, *J. Am. Chem. Soc.*, 2017, **139**, 7761–7767.
10 R. Kircher, J. Xu and D. A. Barskiy, *J. Am. Chem. Soc.*, 2024, **146**, 514–520.
11 A. I. Silva Terra, M. Rossetto, C. L. Dickson, G. Peat, D. Uhrín and M. E. Halse, *ACS Meas. Sci. Au*, 2023, **3**, 73–81.
12 A. I. Silva Terra and M. E. Halse, *Chem.:Methods*, 2025, **5**, e202400094.
13 B. O. Jimmink, M. Negroni, T. B. Posthumus, A. P. M. Kentgens and M. Tessari, *Anal. Chem.*, 2025, **97**, 10962–10965.
14 E. T. Van Dyke, J. Eills, R. Picazo-Frutos, K. F. Sheberstov, Y. Hu, D. Budker and D. A. Barskiy, *Sci. Adv.*, 2022, **8**, eabp9242.
15 S. Alcicek, E. Van Dyke, J. Xu, S. Pustelny and D. A. Barskiy, *Chem.:Methods*, 2023, **3**, e202200075.
16 J. Yang, R. Xin, S. Lehmkuhl, J. G. Korvink and J. J. Brandner, *Sci. Rep.*, 2024, **14**, 21022.
17 F. Ellermann, P. Saul, J.-B. Hövener and A. N. Pravdivtsev, *Anal. Chem.*, 2023, **95**, 6244–6252.
18 S. Fleischer, J. Yang, K. Ausmees, I. Reile, N. MacKinnon, J. G. Korvink and S. Lehmkuhl, *Chem. Commun.*, 2026, **62**, 3342–3346.
19 D. A. Taylor, J. McCall, F. Hill-Casey, J. Hedges, I. Hehir, G. J. Yule, S. Murray, A. Mortimer and M. E. Halse, *Anal. Chem.*, 2026, **98**, 18713–18721.
20 K. Zangger, *Prog. Nucl. Magn. Reson. Spectrosc.*, 2015, **86–87**, 1–20.
21 T. Castaing-Cordier, D. Bouillaud, P. Bowyer, O. Goncalves, P. Giraudeau and J. Farjon, *Chem. Phys. Chem.*, 2019, **20**, 736–744.
22 K. Zangger and H. Sterk, *J. Magn. Reson.*, 1997, **124**, 486–489.
23 A. Lupulescu, G. L. Olsen and L. Frydman, *J. Magn. Reson.*, 2012, **218**, 141–146.
24 P. Kiraly, M. Nilsson and G. A. Morris, *J. Magn. Reson.*, 2018, **293**, 19–27.
25 J. R. Garbow, D. P. Weitekamp and A. Pines, *Chem. Phys. Lett.*, 1982, **93**, 504–509.
26 V. V. Krishnamurthy, *Magn. Reson. Chem.*, 1997, **35**, 9–12.
27 M. Foroozandeh, R. W. Adams, N. J. Meharry, D. Jeannerat, M. Nilsson and G. A. Morris, *Angew. Chem., Int. Ed.*, 2014, **53**, 6990–6992.
28 W. P. Aue, J. Karhan and R. R. Ernst, *J. Chem. Phys.*, 1976, **64**, 4226–4227.
29 J. Mandral, S. Roques, J.-N. Dumez, P. Giraudeau and J. Farjon, *Anal. Methods*, 2025, **17**, 3171–3182.
30 N. H. Meyer and K. Zangger, *Angew. Chem., Int. Ed.*, 2013, **52**, 7143–7146.
31 K. J. Donovan and L. Frydman, *Angew. Chem., Int. Ed.*, 2015, **54**, 594–598.
32 D. A. Taylor, L. S. Natrajan, M. Nilsson and R. W. Adams, *Magn. Reson. Chem.*, 2021, **59**, 1244–1252.
33 P. Kiraly, N. Kern, M. P. Plesniak, M. Nilsson, D. J. Procter, G. A. Morris and R. W. Adams, *Angew. Chem., Int. Ed.*, 2021, **60**, 666–669.
34 A. Jenne, W. Bermel, C. A. Michal, O. Gruschke, R. Soong, R. Ghosh Biswas, M. Bastawrous and A. J. Simpson, *Angew. Chem., Int. Ed.*, 2022, **61**, e202110044.
35 K. Downey, W. Bermel, R. Soong, D. H. Lysak, K. Ronda, K. Steiner, P. M. Costa, W. W. Wolff, V. Decker, F. Busse, B. Goerling, A. Haber, M. J. Simpson and A. J. Simpson, *Magn. Reson. Chem.*, 2024, **62**, 345–360.
36 P. L. Norcott, *Phys. Chem. Chem. Phys.*, 2022, **24**, 13527–13533.
37 P. Kiraly, M. Nilsson, G. A. Morris and R. W. Adams, *Chem. Commun.*, 2021, **57**, 2368–2371.
38 D. A. Taylor, P. Kiraly, P. Bowyer, M. Nilsson, L. Castanar, G. A. Morris and R. W. Adams, *Chem. Commun.*, 2023, **59**, 6734–6737.
39 M. Bazzoni, A. Regheasse, P. Giraudeau, A. Bernard, R. W. Adams, G. A. Morris, M. Nilsson, P. Kiraly and J.-N. Dumez, *Chem. Commun.*, 2026, **62**, 11874–11877.
40 M. R. M. Koos, G. Kummerlowe, L. Kaltschnee, C. M. Thiele and B. Luy, *Angew. Chem., Int. Ed.*, 2016, **55**, 7655–7659.
41 P. J. Rayner, P. Norcott, K. M. Appleby, W. Iali, R. O. John, S. J. Hart, A. C. Whitwood and S. B. Duckett, *Nat. Commun.*, 2018, **9**, 4251.
42 B. J. Tickner, O. Semenova, W. Iali, P. J. Rayner, A. C. Whitwood and S. B. Duckett, *Catal. Sci. Technol.*, 2020, **10**, 1343–1355.
43 W. Iali, P. J. Rayner and S. B. Duckett, *Sci. Adv.*, 2018, **4**, eaao6250.
44 P. M. Richardson, S. Jackson, A. J. Parrott, A. Nordon, S. B. Duckett and M. E. Halse, *Magn. Reson. Chem.*, 2018, **56**, 641–650.
45 P. Sakhaii and W. Bermel, *J. Magn. Reson.*, 2014, **242**, 220–223.
46 H. Geen and R. Freeman, *J. Magn. Reson.*, 1991, **93**, 93–141.
47 J.-N. Dumez, *J. Magn. Reson.*, 2021, **323**, 106817.
48 M. J. Thrippleton and J. Keeler, *Angew. Chem., Int. Ed.*, 2003, **42**, 3938–3941.
49 A. J. Shaka, C. J. Lee and A. Pines, *J. Magn. Reson.*, 1988, **77**, 274–293.